

Full-Color Magnetic Nanoparticles Based on Holmium-Doped Polymers

Kotona Kohaku, Mizuki Inoue, Hirofumi Kanoh, Tatsuo Taniguchi, Keiki Kishikawa, and Michinari Kohri*



Cite This: <https://dx.doi.org/10.1021/acscapm.0c00038>



Read Online

ACCESS |



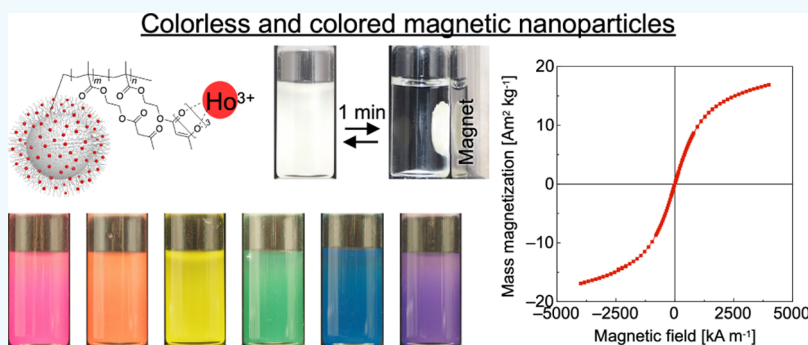
Metrics & More



Article Recommendations



Supporting Information



ABSTRACT: Here, we have demonstrated the production of colorless and full-color magnetic nanoparticles based on holmium (Ho)-doped polymers, which could not be achieved with conventional dark brown iron oxide magnetic nanoparticles. The coordination of Ho, a lanthanide with low colorability and a strong magnetic moment, with a poly(2-acetoacetoxy ethyl methacrylate) brush built on the surface of submicron-sized silica particles allowed for the formation of colorless magnetic nanoparticles. Additionally, bright and full-color magnetic nanoparticles were obtained by mixing different colored magnetic nanoparticles that were prepared by copolymerization of 2-acetoacetoxy ethyl methacrylate and dye monomers. Various colors, including transparency, were demonstrated by means of the present method, which determines the presence or absence of magnetism by Ho doping. The bright and magnetically controllable colored nanoparticles presented herein may have a significant impact on practical substances and applications, such as ink and biomedical and device applications.

KEYWORDS: magnetic materials, holmium, lanthanide, full color, magnetically responsive polymer

INTRODUCTION

Magnetic materials play an important role in the progress of scientific and industrial growth.¹ In previous reports, iron oxide nanoparticles composed of magnetite (Fe_3O_4) and/or maghemite ($\gamma\text{-Fe}_2\text{O}_3$) nanoparticles have been mainly used as a component of magnetic materials because they exhibit excellent magnetic properties.^{2,3} Iron oxide nanoparticles can be easily combined with other materials, such as polymer matrices and inorganic compounds, to produce a variety of functional magnetic composites. Applications of iron oxide nanoparticles and their composites include magnetic resonance imaging, medical diagnostics, memory devices, catalysts, and sensors.^{4–6} While excellent magnetic materials have been created, their use as colored materials and optical materials is limited by the fact that iron oxide nanoparticles are dark brown in color, as shown in Figure S1.⁷ Research into fluorescent magnetic nanoparticles where coloring is not an issue is ongoing,^{8–11} but to our knowledge, there has been little progress in developing bright colored magnetic nanoparticles. In recent years, research on structural colors utilizing the

interaction between nanostructures and light has been conducted.^{12–16} It has also been reported that by using the Fe_3O_4 nanoparticles as a component, the color tone of the structural color can be controlled by a magnetic field.^{17–19} Although it is possible to easily change the color, assembly of particles is required to build a nanostructure that exhibits the structural color. In contrast, colored magnetic nanoparticles can be directly and easily detected visibly without the assembly of particles. While these particles are expected to be used as medical diagnostic materials for magnetic separation, bright colored particles need to be prepared for sensitive detection.^{20,21} In addition, the development of high-resolution color electronic paper driven by a magnetic field requires the

Received: January 9, 2020

Accepted: March 17, 2020

Published: March 17, 2020

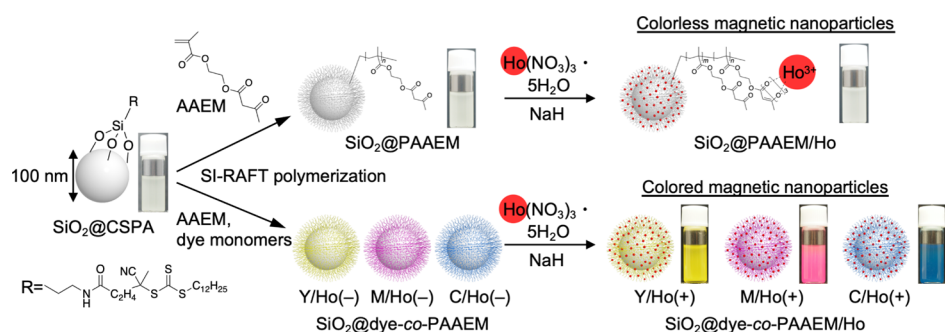


Figure 1. Schematic illustration of the preparation of colorless and colored magnetic nanoparticles functionalized by Ho-doped polymers. The insets show photographs of a glass vial (volume: 2 mL) containing a DMF dispersion of the prepared particles (10 wt %).

production of submicron-sized colored magnetic nanoparticles, which are expected to respond quickly to a magnet.²² However, the dark coloration intensifies as the size of the composite materials decreases, as long as iron oxide nanoparticles are a component. The size of the composite materials is inversely related to the brightness of the coloration. Therefore, for the production of bright colored magnetic materials, significant work remains to be done to develop magnetic nanoparticles that are essentially colorless and have a magnetic response comparable to that of conventional iron oxide magnetic nanoparticles.⁷

Lanthanides exhibit excellent luminescent and magnetic properties due to their shielded 4f orbital electrons because the energy of the 4f orbital is lower than that of the 5d orbital.²³ The luminescent properties of lanthanide complex materials have been well investigated, and lanthanide complex materials have been widely used in industrial applications.^{24–27} Much knowledge about the magnetic properties of lanthanides has also been accumulated. In addition to lanthanide-based permanent magnets,²⁸ lanthanide single-molecule magnets^{29–31} have also attracted considerable attention because of their potential applications, such as in spintronic devices, high-density information storage, and quantum computing. Some lanthanides, for example, terbium (Tb), dysprosium (Dy), holmium (Ho), and erbium (Er) are known to have high magnetic moments,²³ and in recent years, the development of magnetic materials based on the assembly of lanthanide complexes has progressed.^{32,33} We prepared magnetic materials by immobilizing Ho or Tb on poly(acrylic acid)-based polymeric scaffolds.^{34,35} The resulting lanthanide composite materials responded quickly to a magnet without using conventional iron oxide nanoparticles. While not reported previously, these lanthanide composites will essentially be colorless magnetic materials, because lanthanides have low colorability.

Herein, we demonstrated the creation of bright and full-color magnetic nanoparticles based on Ho-doped polymers (Figure 1). Submicron-sized silica (SiO₂) particles (diameter: approximately 100 nm) were decorated with poly(2-acetoacetoxy ethyl methacrylate) (PAAEM) brushes that act as Ho-immobilized scaffolds. Then, Ho was coordinated under alkaline conditions to obtain colorless magnetic nanoparticles (SiO₂@PAAEM/Ho particles). Colored magnetic nanoparticles (SiO₂@dye-co-PAAEM/Ho particles) were prepared by the copolymerization of AAEM and dye monomers. By mixing differently colored nanoparticles, bright and full-color magnetic nanoparticles were formed. To our knowledge, this is the first study to produce bright colored submicron-sized magnetic

nanoparticles, which greatly expand the application range of magnetic materials. This method has a novel feature, in that the presence or absence of magnetism in the particles can be easily controlled by only Ho doping, which provide flexibility in material design.

EXPERIMENTAL SECTION

Materials. Tetrahydrofuran (THF) (>99.5%) was obtained from Kanto Chemical Co., Inc. (Tokyo, Japan). 2,2'-Azobisisobutyronitrile (AIBN) (>98.0%), dichloromethane (DCM) (>99.5%), holmium(III) nitrate pentahydrate [Ho(NO₃)₃·5H₂O] (>99.5%), reactive dye monomers (B01, Y03, and R13), sodium hydride (60% in paraffin oil), hydrochloric acid (HCl), *N,N*-dimethylformamide (DMF) (>99.5%), and 1,4-dioxane (>99.5%) were purchased from Wako Pure Chemical Ind., Ltd. (Osaka, Japan). 3-Aminopropyltrimethoxysilane (APTMS) (>97.0%), *N*-hydroxysuccinimide (NHS) (>98.0%), and 4-cyano-4-[(dodecylsulfanylthiocarbonyl)sulfanyl]pentanoic acid (CSPA) (>97.0%) were purchased from Sigma-Aldrich Japan Co., LLC. (Tokyo, Japan). AAEM (>95.0%), *N,N'*-dicyclohexylcarbodiimide (DCC) (>98.0%), and diethyl ether (>99.5%) were purchased from Tokyo Chemical Ind., Co., Ltd. (Tokyo, Japan). AAEM was purified on an alumina column. Deionized water with a resistance of 18.2 MΩ·cm was obtained by passing water through a Millipore Simplicity UV system. Silica (SiO₂) particles (MP-1040) were supplied by Nissan Chemical Co. (Chiba, Japan), and were purified by stirring in concentrated nitric acid and washing with ultra-pure water, and subsequently with THF. All other chemicals and solvents were of reagent grade, and were used as received.

Measurements. The Fourier transform infrared (FT-IR) spectra were recorded using a JASCO FT/IR-420 instrument. Transmission electron microscopy (TEM) and energy dispersive X-ray spectrometry (EDS) mapping were performed on a Hitachi H-7650 instrument operated at 100 kV. The dynamic light scattering (DLS) measurements were performed with a Malvern Zetasizer Nano ZS system. The X-ray photoelectron spectroscopy (XPS) measurements were performed using a JEOL JPS-9030 instrument. Inductively coupled plasma atomic emission spectroscopy (ICP-AES) analysis was performed using a PerkinElmer Optima8300 instrument. The magnetic properties were measured using a Quantum Design MPMS XL-5 superconducting quantum interference device (SQUID) magnetometer. The ultraviolet–visible (UV–vis) absorption spectra were obtained using a Hitachi U-3010 spectrophotometer. The gel permeation chromatography (GPC) measurements were performed on a Tosoh HLC-8220GPC system equipped with a refractive index detector, and THF was used as a mobile phase and introduced with a flow rate of 0.3 mL min⁻¹ at 40 °C on serially combined TSKgel SuperHZM-N, SuperHZ2500, and SuperHZ1000 columns. Calibration was carried out using polymethylmethacrylate standards. The grafting density of the polymer brushes was investigated using a Shimadzu DTG-60A thermogravimetry/differential thermal analysis (TG-DTA) instrument. Photographs of the samples were taken using an Olympus OM-D digital camera.

Preparation of SiO₂@PAAEM Particles. The mixture of a silane coupling reagent, APTMS (4.6 g, 26 mmol), and SiO₂ particles (10 g) was stirred under reflux for 12 h in THF, affording amino-functionalized SiO₂ particles (SiO₂@APTMS; 4.54 groups nm⁻²). SiO₂@APTMS (9.0 g) was then added to 300 mL of DCM containing CSPA (3.0 g, 7.4 mmol), NHS (1.7 g, 15 mmol), and DCC (3.0 g, 15 mmol). The mixtures were allowed to react at 25 °C for 24 h in the dark, giving rise to CSPA-modified SiO₂ particles (SiO₂@CSPA; 2.46 groups nm⁻²). The prepared SiO₂@CSPA particles were immersed in a 50 mL flask containing 20 mL of 1,4-dioxane with the AAEM monomer (2.33 g, 10.9 mmol), CSPA (22 mg, 0.054 mmol), and AIBN (1.8 mg, 0.010 mmol), which was degassed through three freeze–pump–thaw cycles, and then polymerization was performed at 70 °C. After 18 h, the polymerization process was quenched by cooling in an ice bath, and the particles were purified repeatedly by centrifugation (10,000 rpm for 10 min) and redispersion, forming PAAEM-grafted SiO₂ particles (SiO₂@PAAEM; 0.16 chains nm⁻²).

Preparation of SiO₂@dye-co-PAAEM Particles. Colored PAAEM-grafted SiO₂ particles were prepared by the copolymerization of AAEM and dye monomers (B01, Y03, or R13: 0.65 wt % relative to AAEM), and were designated as SiO₂@dye-co-PAAEM particles.

Preparation of Colorless and Colored Magnetic Particles. Sodium hydride (2.6 mg, 0.11 mmol) and Ho(NO₃)₃·5H₂O (0.049 g, 0.11 mmol) were added to SiO₂@PAAEM (0.22 g, 0.32 mmol) dispersed in THF. The mixtures were stirred at room temperature. After 24 h, the particles were purified repeatedly by centrifugation (10,000 rpm for 10 min) and redispersion, producing colorless magnetic particles (SiO₂@PAAEM/Ho). Colored magnetic particles instead of SiO₂@PAAEM particles were prepared using SiO₂@dye-co-PAAEM.

RESULTS AND DISCUSSION

SiO₂@PAAEM particles were prepared by the surface-initiated reversible addition–fragmentation chain transfer polymerization of AAEM on the surface of SiO₂ particles. The volume-average diameters of the SiO₂@PAAEM particles in DMF, as measured using DLS, were approximately 122 nm, which is larger than the approximately 100 nm diameter core SiO₂@CSPA particles, indicating that the SiO₂@PAAEM particles have PAAEM shell layers with approximately 11 nm thickness (Figure S2). TEM analysis of the SiO₂@PAAEM particles also suggested the formation of PAAEM layers with approximately 14 nm thickness (Figure S3). The grafting density of the PAAEM shell calculated by TG-DTA was approximately 0.16 chains nm⁻², and the number-average molecular weight of PAAEM measured by GPC was approximately 30,900, indicating that the surfaces of the SiO₂ particles were coated with highly densely packed PAAEM brushes (Figures S4 and S5).

The SiO₂@PAAEM/Ho particles were prepared by doping Ho on the PAAEM brushes. The immobilization of Ho was measured by FT-IR spectroscopy (Figure 2a). The strong absorption bands at 1723 and 1632 cm⁻¹ in the spectra of the SiO₂@PAAEM particles were attributed to the stretching vibrations of C=O and C=C (enol isomer), respectively, in the β-diketone groups. The redshift of the bands at 1723 and 1632 to 1719 and 1625 cm⁻¹ in the spectra of the SiO₂@PAAEM/Ho particles indicated the coordination of the carbonyl group to the Ho cation, which agrees with the report that the peak attributed to the carbonyl groups redshifted after the binding of the lanthanide ion to the β-diketone groups.³⁶ The peak attributed to C=C vibrations was redshifted to 1625 cm⁻¹ after the deprotonation of the enol hydroxyl group. While a more detailed analysis of the complex form is required, these data suggest that trivalent Ho complexed with the β-diketone group of AAEM, as shown in Figure 2b.^{37,38} The Ho_{4d} XPS

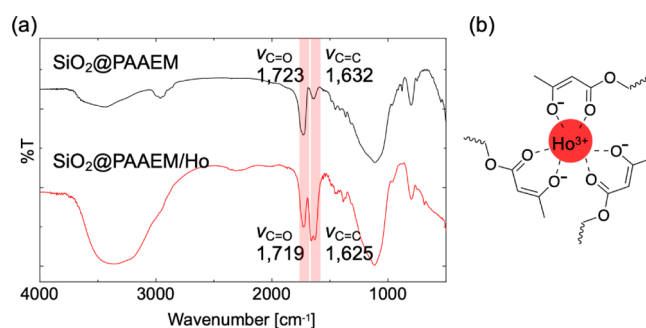


Figure 2. (a) FT-IR spectra of SiO₂@PAAEM and SiO₂@PAAEM/Ho particles. (b) Proposed structure of the complex of Ho and AAEM.

data for the SiO₂@PAAEM/Ho particles show the introduction of Ho (Figure S6). Additionally, the introduction of Ho was confirmed by the results of TEM–EDS mapping of the SiO₂@PAAEM/Ho particles (Figure S7). The DLS measurements were performed in DMF to investigate the dispersion stability of the SiO₂@PAAEM/Ho particles (Figure S8). Although the formation of secondary particles, which may be caused by Ho, was suggested, the obtained particles were well dispersed in the solvent, and no noticeable aggregation was observed.

Figures S9 and 3a show photographs of the DMF dispersion of SiO₂@CSPA, SiO₂@PAAEM, and SiO₂@PAAEM/Ho

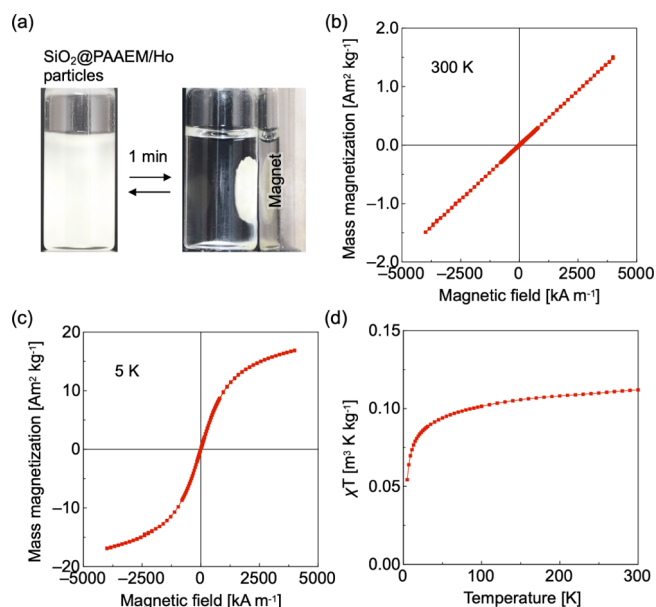


Figure 3. (a) Digital photographs of the magnetically responsive behavior of SiO₂@PAAEM/Ho particles. Magnetization curve of SiO₂@PAAEM/Ho particles at (b) 300 K and (c) at 5 K in an applied magnetic field up to 3979 kA m⁻¹ (5 T). (d) Temperature dependence of χT at 795.8 kA m⁻¹ (1 T) for SiO₂@PAAEM/Ho particles.

particles. As seen from these photographs, no coloration was observed, neither after the formation of the PAAEM brushes nor after the immobilization of Ho. As shown in Figure S10, no absorption other than absorption due to particle scattering was obtained, indicating the production of colorless particles. A neodymium magnet (1 T) was placed on the side of a glass vial, in which each particle was dispersed and allowed to stand.

Although the $\text{SiO}_2\text{@CSPA}$ and $\text{SiO}_2\text{@PAAEM}$ particles did not respond to the magnet after 1 h (Figure S9), the $\text{SiO}_2\text{@PAAEM}/\text{Ho}$ particles were attracted immediately after the placement of the magnet, and almost all of the particles were collected at the magnet after 1 min (Figure 3a). The collected $\text{SiO}_2\text{@PAAEM}/\text{Ho}$ particles were easily redispersed in solution when the magnet was removed. The detailed magnetic field response measurements of the bare SiO_2 , $\text{SiO}_2\text{@PAAEM}$, and $\text{SiO}_2\text{@PAAEM}/\text{Ho}$ particles were performed with a SQUID magnetometer with fields of up to 3979 kA m^{-1} (5 T). The results were obtained by the conventional magnetic hysteresis loop measurement technique. First, the mass magnetization at 300 K was measured because it is assumed that the polymer-based magnetic composite materials are mainly used near room temperature. While the magnetic response of the bare SiO_2 and $\text{SiO}_2\text{@PAAEM}$ particles was very small (Figure S11), the mass magnetization of the $\text{SiO}_2\text{@PAAEM}/\text{Ho}$ particles at 3979 kA m^{-1} (5 T) was approximately $1.51 \text{ A m}^2 \text{ kg}^{-1}$ (Figure 3b). As shown in Figure 3c, the $\text{SiO}_2\text{@PAAEM}/\text{Ho}$ particles showed a higher mass magnetization value (approximately $16.9 \text{ A m}^2 \text{ kg}^{-1}$) at 5 K than at 300 K. While saturation magnetization was observed in the measurement made at 5 K, no hysteresis was observed, indicating the paramagnetic property of the sample (Figure 3c).^{34,39,40} The temperature-dependent magnetic properties of the $\text{SiO}_2\text{@PAAEM}/\text{Ho}$ particles were measured at 795.8 kA m^{-1} (1 T) in the temperature range of 5–300 K. The χT versus T plots are shown in Figure 3d. The χT values decreased continuously with cooling. This result also indicated that the sample showed a paramagnetic property. The Ho-immobilized particles had a high mass magnetization and rapidly responded to the neodymium magnet. More importantly, the submicron-sized magnetic nanoparticles prepared by the present method were colorless materials, unlike conventional iron oxide magnetic nanoparticles. The development of colorless nanoparticles, each with magnetic properties, is useful for applications in inks such as magnetic inks and inks for anti-counterfeit materials. These studies are currently underway in our laboratory.

Colored nanoparticles were prepared by the copolymerization of AAEM and dye monomers (Figure 1). The colored magnetic nanoparticles were then prepared by doping Ho onto the $\text{SiO}_2\text{@dye-co-PAAEM}$ particles. The yellow-, magenta-, and cyan-colored magnetic nanoparticles were named Y/Ho(+), M/Ho(+), and C/Ho(+) particles, respectively. The colored nanoparticles before doping Ho were named Y/Ho(-), M/Ho(-), and C/Ho(-) particles. The obtained colored nanoparticles showed maximum absorption at 450, 560, and 625 nm, corresponding to the respective colors (Figure 4a). While the colored magnetic nanoparticles dispersed in DMF had slightly slower responses to the neodymium magnet than the colorless magnetic nanoparticles, almost all of the particles were collected at the magnet after 5 min (Figure 4b). The mass magnetism of the colored magnetic nanoparticles at 300 K was lower than that of the colorless magnetic nanoparticles (Figure 5a). Ho immobilized on the particle surface was recovered by an acid treatment (0.1 M HCl), and the amount of Ho was measured by ICP-AES. As shown in Figure 5b, the amount of Ho immobilized on the colorless particles was larger than the amount carried by the colored particles. This phenomenon probably occurred because the amount of Ho immobilized onto the colored particles was reduced by the introduction of dye monomers

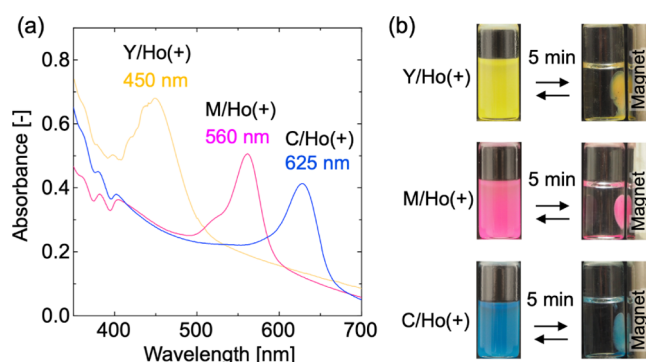


Figure 4. (a) Absorption spectra of colored magnetic nanoparticles. (b) Digital photographs of the magnetically responsive behavior of colored magnetic nanoparticles.

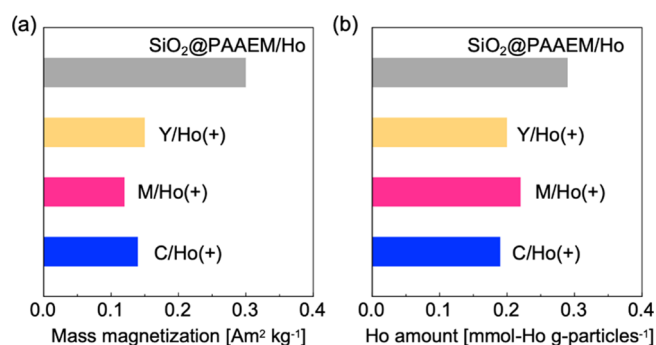


Figure 5. (a) Mass magnetization of the $\text{SiO}_2\text{@PAAEM}/\text{Ho}$ and colored magnetic particles measured at 795.8 kA m^{-1} (1 T). (b) Amount of Ho on the $\text{SiO}_2\text{@PAAEM}/\text{Ho}$ and colored magnetic nanoparticles, as measured by ICP-AES.

into the PAAEM brushes. While controlling the amount of Ho immobilized by the stricter design of the polymer brushes is a future task, we obtained bright colored magnetic nanoparticles that responded to a magnetic field.

The creation of magnetic nanoparticles with various colors was investigated by mixing the three primary colored magnetic nanoparticles (Figure 6a). When the Y/Ho(+) and M/Ho(+) particles were mixed in a 1:1 ratio, orange-colored magnetic nanoparticles were easily obtained. Purple- and green-colored magnetic nanoparticles were also obtained by simply mixing M/Ho(+) with the C/Ho(+) particles and Y/Ho(+) with the C/Ho(+) particles, respectively. From the absorption spectra of the orange-, purple-, and green-colored magnetic nanoparticles shown in Figure 6b, the spectra corresponding to the absorption of the combined two-colored particles were obtained. By controlling the mixing of the two differently colored particles, we successfully obtained a variety of colored magnetic nanoparticles. Figure 6a shows the International Commission on Illumination (CIE) 1931 chromaticity diagram, and the colors of each sample are plotted. These data clearly indicate that the present method enables producing nearly the full range of colored magnetic nanoparticles.

It should be noted that the presence or absence of magnetism of the particles prepared by this method can be easily controlled by whether or not Ho is immobilized. Magnetic color tuning was investigated by combining the four particles, that is, the Y/Ho(+), Y/Ho(-), C/Ho(+), and C/Ho(-) particles (Figure 6c). Mixing of Y/[Ho(+)] or Ho(-)]

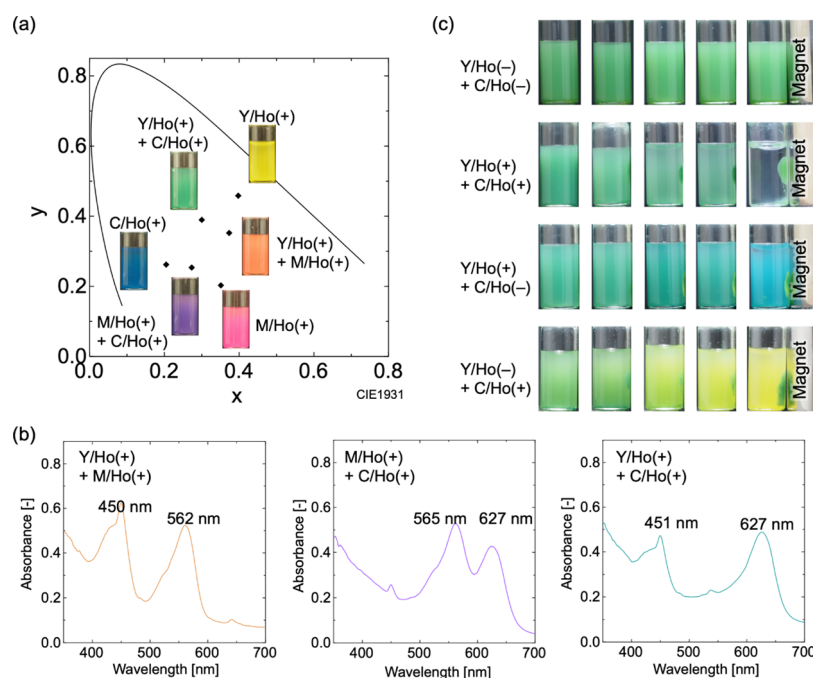


Figure 6. (a) CIE chromaticity plot of colors prepared by particle mixing. The photographs show the DMF dispersion of particles (10 wt %). (b) Absorption spectra of orange- [Y/Ho(+) and M/Ho(+)], purple- [M/Ho(+) and C/Ho(+)], and green- [Y/Ho(+) and C/Ho(+)] colored magnetic nanoparticles. (c) Digital photographs showing the color change achieved by mixing the Y/[Ho(+) or Ho(-)] and C/[Ho(+) or Ho(-)] particles.

and C/[Ho(+) or Ho(-)] particles led to the formation of green-colored particles. However, the response behavior to the magnet varied greatly depending on the combination of particles. When the neodymium magnet was placed in a DMF dispersion containing Y/Ho(-) and C/Ho(-) particles, the particles remained dispersed, and the solution remained a green color. The dispersion of the Y/Ho(+) and C/Ho(+) particles containing Ho responded to the magnet quickly, and finally, the solution became transparent. If either particle contained Ho, only the Ho-doped particles responded to the magnet. When the Y/Ho(+) and C/Ho(-) particles were combined, only the Y/Ho(+) particles were attracted to the magnet, and the color of the solution became orange because of the dispersed C/Ho(-) particles. In contrast, when the Y/Ho(-) particles and C/Ho(+) particles were combined, the Y/Ho(-) particles remained in the solution phase and the C/Ho(+) particles were attracted to the magnet, resulting in a yellow solution color. When the Ho-containing particles and particles not containing Ho are mixed, it is possible that Ho exchanges between the particles. Thus, after collecting the C/Ho(+) particles with the magnet, the Y/Ho(-) particles in the solution phase were collected, and the amount of Ho was measured by ICP-AES. Almost no signal from Ho was detected (data not shown). Under these experimental conditions, there was no movement of Ho between the particles, indicating that the obtained magnetic particles were stable in solution. Various colors, including transparency, can be expressed depending on the presence or absence of Ho doped on particles under a magnetic field.

By immobilizing Ho onto PAAEM brushes and having a strong magnetic moment, we succeeded in producing a new category of magnetic nanoparticles that respond quickly to a magnet. Because particles are formed by the coordination of Ho with the PAAEM brushes, Ho desorbs and loses its magnetism under acidic conditions. However, it has become

possible to develop colorless magnetic nanoparticles that cannot be achieved with conventional iron oxide magnetic nanoparticles. In addition, utilizing the colorless features, bright and full-color magnetic nanoparticles were produced. Through functionalization by modification of the particle surface, the development of a wide variety of applications, including use in ink, medical, and device applications, will be expected.

CONCLUSIONS

In conclusion, we demonstrated the preparation of colorless magnetic nanoparticles utilizing the properties of lanthanides with low colorability and high magnetic moment. The submicron-sized SiO₂ particles decorated with Ho-doped polymer brushes were almost colorless and responded quickly to a magnet. The resulting colorless magnetic nanoparticles disperse well in solvents and are almost invisible to the human eye, making them useful for applications such as magnetic inks and anticounterfeit materials. Using these colorless properties, we also succeeded in obtaining bright colored magnetic nanoparticles by copolymerizing dye monomers in PAAEM brushes. By mixing three primary colored magnetic particles, that is, Y/Ho(+), M/Ho(+), and C/Ho(+) particles, full-color magnetic nanoparticles were also developed. While it has been difficult to prepare highly colored submicron-sized magnetic nanoparticles using conventional iron oxide magnetic nanoparticles with deep coloration, this study made this preparation easy. Additionally, in this system, control of various colors, including the generation of transparency, was possible because the presence or absence of magnetism can be easily controlled by Ho doping. This simple and novel process using Ho-doped polymers, combined with particle surface modification technology, will be useful for practical applications, such as medical diagnostic materials utilizing magnetic separation and color electronic paper driven by magnetic fields.

■ ASSOCIATED CONTENT

SI Supporting Information

The Supporting Information is available free of charge at <https://pubs.acs.org/doi/10.1021/acsapm.0c00038>.

Additional experimental details including a photograph of particles and the results of DLS, TEM, TGA, GPC, XPS, TEM-EDS, UV-vis, and magnetization measurements (PDF)

■ AUTHOR INFORMATION

Corresponding Author

Michinari Kohri – Department of Applied Chemistry and Biotechnology, Graduate School of Engineering, Chiba University, Inage-ku, Chiba 263-8522, Japan; orcid.org/0000-0003-1118-5568; Email: kohri@faculty.chiba-u.jp

Authors

Kotona Kohaku – Department of Applied Chemistry and Biotechnology, Graduate School of Engineering, Chiba University, Inage-ku, Chiba 263-8522, Japan

Mizuki Inoue – Department of Chemistry, Graduate School of Science, Chiba University, Inage-ku, Chiba 263-8522, Japan

Hirofumi Kanoh – Department of Chemistry, Graduate School of Science, Chiba University, Inage-ku, Chiba 263-8522, Japan; orcid.org/0000-0003-1696-5432

Tatsuo Taniguchi – Department of Applied Chemistry and Biotechnology, Graduate School of Engineering, Chiba University, Inage-ku, Chiba 263-8522, Japan

Keiki Kishikawa – Department of Applied Chemistry and Biotechnology, Graduate School of Engineering, Chiba University, Inage-ku, Chiba 263-8522, Japan; orcid.org/0000-0002-7539-568X

Complete contact information is available at: <https://pubs.acs.org/doi/10.1021/acsapm.0c00038>

Notes

The authors declare no competing financial interest.

■ ACKNOWLEDGMENTS

M.K. acknowledges the support of JSPS KAKENHI (grant numbers: 16K14072 and 19K22213), the Hosokawa Powder Technology Foundation, the Asahi Glass Foundation, and the Ogasawara Foundation for the Promotion of Science & Engineering. We would like to thank Prof. Kyoichi Saito and Shoko Naruke of Chiba University for the ICP-AES measurements. We acknowledge Nissan Chemical Co. for providing the silica particles. The XPS measurements were performed at the Center for Analytical Instrumentation and the Chiba Iodine Resource Innovation Center (CIRIC), Chiba University.

■ REFERENCES

- (1) Gutfleisch, O.; Willard, M. A.; Brück, E.; Chen, C. H.; Sankar, S. G.; Liu, J. P. Magnetic Materials and Devices for the 21st Century: Stronger, Lighter, and More Energy Efficient. *Adv. Mater.* **2011**, *23*, 821–842.
- (2) Laurent, S.; Forge, D.; Port, M.; Roch, A.; Robic, C.; Vander Elst, L.; Muller, R. N. Magnetic Iron Oxide Nanoparticles: Synthesis, Stabilization, Vectorization, Physicochemical Characterizations, and Biological Applications. *Chem. Rev.* **2008**, *108*, 2064–2110.
- (3) Thévenot, J.; Oliveira, H.; Sandre, O.; Lecommandoux, S. Magnetic Responsive Polymer Composite Materials. *Chem. Soc. Rev.* **2013**, *42*, 7099–7116.
- (4) Shinkai, M. Functional Magnetic Particles for Medical Application. *J. Biosci. Bioeng.* **2002**, *94*, 606–613.
- (5) Sangaiya, P.; Jayaprakash, R. A Review on Iron Oxide Nanoparticles and Their Biomedical Applications. *J. Supercond. Novel Magn.* **2018**, *31*, 3397–3413.
- (6) Medeiros, S. F.; Santos, A. M.; Fessi, H.; Elaissari, A. Stimuli-Responsive Magnetic Particles for Biomedical Applications. *Int. J. Pharm.* **2011**, *403*, 139–161.
- (7) Kobayashi, N.; Masumoto, H.; Takahashi, S.; Maekawa, S. Optically Transparent Ferromagnetic Nanogranular Films with Tunable Transmittance. *Sci. Rep.* **2016**, *6*, 34227.
- (8) Kim, J.; Kim, H. S.; Lee, N.; Kim, T.; Kim, H.; Yu, T.; Song, I. C.; Moon, W. K.; Hyeon, T. Multifunctional Uniform Nanoparticles Composed of a Magnetite Nanocrystal Core and a Mesoporous Silica Shell for Magnetic Resonance and Fluorescence Imaging and for Drug Delivery. *Angew. Chem., Int. Ed.* **2008**, *120*, 8566–8569.
- (9) Lin, Y.-S.; Haynes, C. L. Synthesis and Characterization of Biocompatible and Size-Tunable Multifunctional Porous Silica Nanoparticles. *Chem. Mater.* **2009**, *21*, 3979–3986.
- (10) Lone, S.; Cheong, I. W. Fabrication of polymeric Janus particles by droplet microfluidics. *RSC Adv.* **2014**, *4*, 13322–13333.
- (11) Zhu, X.; Zhou, J.; Chen, M.; Shi, M.; Feng, W.; Li, F. Core-shell Fe₃O₄@NaLuF₄: Yb, Er/Tm Nanostructure for MRI, CT and Upconversion Luminescence Tri-modality Imaging. *Biomaterials* **2012**, *33*, 4618–4627.
- (12) Wang, H.; Liu, Y.; Chen, Z.; Sun, L.; Zhao, Y. Anisotropic Structural Color Particles from Colloidal Phase Separation. *Sci. Adv.* **2020**, *6*, No. eaay1438.
- (13) Shang, L.; Zhang, W.; Xu, K.; Zhao, Y. Bio-Inspired Intelligent Structural Color Materials. *Mater. Horiz.* **2019**, *6*, 945–958.
- (14) Goerlitzer, E. S. A.; Klupp Taylor, R. N.; Vogel, N. Bioinspired Photonic Pigments from Colloidal Self-Assembly. *Adv. Mater.* **2018**, *30*, 1706654.
- (15) Kohri, M.; Nannichi, Y.; Taniguchi, T.; Kishikawa, K. Biomimetic Non-Iridescent Structural Color Materials from Polydopamine Black Particles that Mimic Melanin Granules. *J. Mater. Chem. C* **2015**, *3*, 720–724.
- (16) Kawamura, A.; Kohri, M.; Morimoto, G.; Nannichi, Y.; Taniguchi, T.; Kishikawa, K. Full-Color Biomimetic Photonic Materials with Iridescent and Non-Iridescent Structural Colors. *Sci. Rep.* **2016**, *6*, 33984.
- (17) He, L.; Wang, M.; Ge, J.; Yin, Y. Magnetic Assembly Route to Colloidal Responsive Photonic Nanostructures. *Acc. Chem. Res.* **2012**, *45*, 1431–1440.
- (18) Teshima, M.; Seki, T.; Takeoka, Y. Simple Preparation of Magnetic Field-Responsive Structural Colored Janus Particles. *Chem. Commun.* **2018**, *54*, 2607–2610.
- (19) Chi, J.; Shao, C.; Zhang, Y.; Ni, D.; Kong, T.; Zhao, Y. Magnetically Responsive Colloidal Crystals with Angle-Independent Gradient Structural Colors in Microfluidic Droplet Arrays. *Nanoscale* **2019**, *11*, 12898–12904.
- (20) Sun, Q.; Zhao, G.; Dou, W. Blue Silica Nanoparticle-Based Colorimetric Immunoassay for Detection of Salmonella Pullorum. *Anal. Methods* **2015**, *7*, 8647–8654.
- (21) Zhu, C.; Zhao, G.; Dou, W. Immunochromatographic Assay Using Brightly Colored Silica Nanoparticles as Visible Label for Point-Of-Care Detection of Clenbuterol. *Sens. Actuators, B* **2018**, *266*, 392–399.
- (22) Yabu, H. Colored Magnetic Janus Particles. *IEICE Trans. Electron.* **2017**, *E100.C*, 955–957.
- (23) Qin, X.; Liu, X.; Huang, W.; Bettinelli, M.; Liu, X. Lanthanide-Activated Phosphors Based on 4f-5d Optical Transitions: Theoretical and Experimental Aspects. *Chem. Rev.* **2017**, *117*, 4488–4527.
- (24) Binnemans, K. Lanthanide-Based Luminescent Hybrid Materials. *Chem. Rev.* **2009**, *109*, 4283–4374.
- (25) Bünzli, J.-C. G. Lanthanide Luminescence for Biomedical Analyses and Imaging. *Chem. Rev.* **2010**, *110*, 2729–2755.

- (26) Hasegawa, Y.; Kitagawa, Y.; Nakanishi, T. Effective Photosensitized, Electrosensitized, and Mechanosensitized Luminescence of Lanthanide Complexes. *NPG Asia Mater.* **2018**, *10*, 52–70.
- (27) Hasegawa, Y.; Kitagawa, Y. Thermo-Sensitive Luminescence of Lanthanide Complexes, Clusters, Coordination Polymers and Metal-Organic Frameworks with Organic Photosensitizers. *J. Mater. Chem. C* **2019**, *7*, 7494–7511.
- (28) Leventis, N.; Gao, X. Nd-Fe-B Permanent Magnet Electrodes. Theoretical Evaluation and Experimental Demonstration of the Paramagnetic Body Forces. *J. Am. Chem. Soc.* **2002**, *124*, 1079–1088.
- (29) Woodruff, D. N.; Winpenny, R. E. P.; Layfield, R. A. Lanthanide Single-Molecule Magnets. *Chem. Rev.* **2013**, *113*, 5110–5148.
- (30) Lu, J.; Guo, M.; Tang, J. Recent Developments in Lanthanide Single-Molecule Magnets. *Chem.–Asian J.* **2017**, *12*, 2772–2779.
- (31) Cosquer, G.; Shen, Y.; Almeida, M.; Yamashita, M. Conducting Single-Molecule Magnet Materials. *Dalton Trans.* **2018**, *47*, 7616–7627.
- (32) Cui, J.; Zhang, G.; Xin, L.; Yun, P.; Yan, Y.; Su, F. Functional Nanoscale Metal-Organic Particles Synthesized from a New Vinyl-imidazole-Based Polymeric Ligand and Dysprosium Ions. *J. Mater. Chem. C* **2018**, *6*, 280–289.
- (33) Brown, P.; Khan, A. M.; Armstrong, J. P. K.; Perriman, A. W.; Butts, C. P.; Eastoe, J. Magnetizing DNA and Proteins Using Responsive Surfactants. *Adv. Mater.* **2012**, *24*, 6244–6247.
- (34) Kohri, M.; Yanagimoto, K.; Kohaku, K.; Shiimoto, S.; Kobayashi, M.; Imai, A.; Shiba, F.; Taniguchi, T.; Kishikawa, K. Magnetically Responsive Polymer Network Constructed by Poly(acrylic acid) and Holmium. *Macromolecules* **2018**, *51*, 6740–6745.
- (35) Kohri, M.; Aoki, Y.; Kohaku, K.; Kishikawa, K. Nanogel Particle-Based Lanthanide Composites for Transparent Magnetic Materials. *Mater. Lett.* **2019**, *254*, 278–281.
- (36) Cao, F.; Huang, T.; Wang, Y.; Liu, F.; Chen, L.; Ling, J.; Sun, J. Novel Lanthanide-Polymer Complexes for Dye-Free Dual Modal Probes for MRI and Fluorescence Imaging. *Polym. Chem.* **2015**, *6*, 7949–7957.
- (37) Zhang, W.; Martinelli, J.; Mayer, F.; Bonnet, C. S.; Szeremeta, F.; Djanashvili, K. Molecular Architecture Control in Synthesis of Spherical Ln-containing Nanoparticles. *RSC Adv.* **2015**, *5*, 69861–69869.
- (38) Binnemans, K. Lanthanide-Based Luminescent Hybrid Materials. *Chem. Rev.* **2009**, *109*, 4283–4374.
- (39) Choudhury, B.; Verma, R.; Choudhury, A. Oxygen Defect Assisted Paramagnetic to Ferromagnetic Conversion in Fe Doped TiO₂ Nanoparticles. *RSC Adv.* **2014**, *4*, 29314–29323.
- (40) Plouffe, B. D.; Murthy, S. K.; Lewis, L. H. Fundamentals and Application of Magnetic Particles in Cell Isolation and Enrichment. *Rep. Prog. Phys.* **2015**, *78*, 016601.